THE JOURNAL OF BIOLOGICAL CHEMISTRY
Vol. 279, No. 14, Issue of April 2, pp. 14264–14272, 2004
Printed in U.S.A.

Evidence of an Intramolecular Interaction between the Two Domains of the BlaR1 Penicillin Receptor during the Signal Transduction*

Received for publication, December 10, 2003, and in revised form, January 20, 2004
Published, JBC Papers in Press, January 21, 2004, DOI 10.1074/jbc.M313488200

Sophie Hanique‡§, Maria-Luigi Colombo‡§, Erik Goormaghtigh¶‖, Patrice Soumillion‡‡, Jean-Marie Frère‡, and Bernard Joris‡ ‡‡§§**

*From the ‡Centre d'Ingénierie des Protéines, Institut de Chimie, Université de Liège, B-4000 Sart-Tilman, ¶Laboratory for the Structure and Function of Biological Membranes, Center for Structural Biology and Bioinformatics, Université Libre de Bruxelles, B-1050 Bruxelles, and **Institut des Sciences de la Vie, Laboratoire de Biochimie Physique et des Biopolymères, Université Catholique de Louvain, B-1348 Louvain-la-Neuve, Belgium*

The BlaR1 protein is a penicillin-sensory transducer involved in the induction of the *Bacillus licheniformis* β-lactamase. The amino-terminal domain of the protein exhibits four transmembrane segments (TM1–TM4) that form a four-α-helix bundle embedded in the plasma bilayer. The carboxyl-terminal domain of 250 amino acids (BlaR-CTD) fused at the carboxyl end of TM4 possesses the amino acid sequence signature of penicillin-binding proteins. This membrane topology suggests that BlaR-CTD and the BlaR-amino-terminal domain are responsible for signal reception and signal transduction, respectively. With the use of phage display experiments, we highlight herein an interaction between BlaR-CTD and the extracellular, 63-amino acid L2 loop connecting TM2 and TM3. This interaction does not occur in the presence of penicillin. This result suggests that binding of the antibiotic to BlaR1 might entail the release of the interaction between L2 and BlaR-CTD, causing a motion of the α-helix bundle and transfer of the information to the cytoplasm of the cell. In addition, fluorescence spectroscopy, CD, and Fourier transform IR spectroscopy experiments indicate that in contrast to the behavior of the corresponding *Staphylococcus aureus* protein, the β-lactam antibiotic does not induce a drastic conformational change in *B. licheniformis* BlaR-CTD.

Bacillus licheniformis 749/I and *Staphyloccocus aureus* PC1 secrete BlaP and BlaZ β-lactamases, respectively, the synthesis of which is induced by the presence of an exogenous β-lactam antibiotic, the inducer (1, 2). In both strains, at least three regulatory genes, *blaI*, *blaR*1, and *blaR*2, are involved in the derepression of the *blaP* or *blaZ* genes. The *blaI* gene encodes a cytoplasmic repressor that, in the absence of antibiotic, maintains a low level of β-lactamase expression (3, 4). The *blaR*1 gene encodes a penicillin sensory transducer (5, 6). The additional regulatory gene, *blaR*2, is not yet identified, but it is believed to play an essential role in the signal transfer process (7, 8). Some *S. aureus* strains have become resistant to β-lactam antibiotics by recruiting an alternative penicillin-binding protein 2′ (PBP2′ or MecA protein),[1] which is much less sensitive than the endogenous PBP targets (4). This low-affinity PBP2′ is under the control of the MecI and MecR1 proteins, which exhibit a high degree of primary structure similarity with the corresponding *S. aureus* and *B. licheniformis* BlaI and BlaR1 β-lactamase regulators. Recently, the tridimensional structures of the *S. aureus* MecI and the N-terminal DNA-binding domain of the *B. licheniformis* BlaI repressors have been solved; as expected, they share the same fold (9, 10). It has been also shown that *S. aureus* MecI and BlaI can be exchanged *in vivo* (11) and that *B. licheniformis* BlaI can recognize the *S. aureus* BlaI DNA operator in a band-shift assay (9). For these reasons, it is believed that the three induction mechanisms are very similar in the two strains.

During the induction of the BlaP/BlaZ β-lactamase or the PBP2′ by β-lactam antibiotics, because these antibiotics do not cross the cytoplasmic membrane, the presence of the antibiotic outside the cell must generate an extracellular event that is transmitted inside the cell to allow the expression of the resistance gene. In the cases of *B. licheniformis* and *S. aureus*, the membrane-bound BlaR1/MecR1 protein plays this role. The membrane topology of *B. licheniformis* BlaR1 (601 amino acid residues) has been determined. It is organized as a two-domain protein, including an N-terminal domain (BlaR-NTD, from residues 1 to 350) anchored into the membrane and an extracellular C-terminal domain (BlaR-CTD, from residues 351 to 601) (12) (Fig. 1*A*). This module belongs to the serine penicillin-recognizing protein family and can be overproduced in *Escherichia coli* as a water-soluble moiety that is efficiently acylated by penicillin and other β-lactam antibiotics (Fig. 1*B*) (13, 14). The second-order acylation rate constants k_2/K' ranged from 0.0017 to more than 1 μM^{-1} s^{-1}, and the deacylation rate constants (k_3) were lower than 4×10^{-5} s^{-1}. These values imply a rapid to very rapid formation of stable acylated adduct. The same result has been obtained for the *S. aureus* BlaR1 protein (15, 16). BlaR-NTD is embedded in the plasma membrane via four transmembrane segments (TM1, TM2, TM3,

* This work was supported in part by the Belgian Program of Interuniversity Poles of Attraction (P5/33) and the Fonds de la Recherche Fondamentale et Collective, Brussels, Belgium (2.4530.03). The costs of publication of this article were defrayed in part by the payment of page charges. This article must therefore be hereby marked "*advertisement*" in accordance with 18 U.S.C. Section 1734 solely to indicate this fact.

§ Both authors contributed equally to this work. Fellows of the Fonds pour la Formation à la Recherche dans l'Industrie et l'Agriculture (Brussels, Belgium).

‖ Research Director, Fonds National de la Recherche Scientifique (Brussels, Belgium).

‡‡ Research Associates, Fonds National de la Recherche Scientifique (Brussels, Belgium).

§§ To whom correspondence should be addressed. Tel.: 0032-4-366-29-54; Fax: 0032-4-366-33-64; E-mail: bjoris@ulg.ac.be.

[1] The abbreviations used are: PBP, penicillin-binding protein; NTD, amino-terminal domain; CTD, carboxyl-terminal domain; TM, transmembrane; ELISA, enzyme-linked immunosorbent assay; PBS, phosphate-buffered saline; 6-APA, 6-aminopenicillanic acid; FT, Fourier transform.

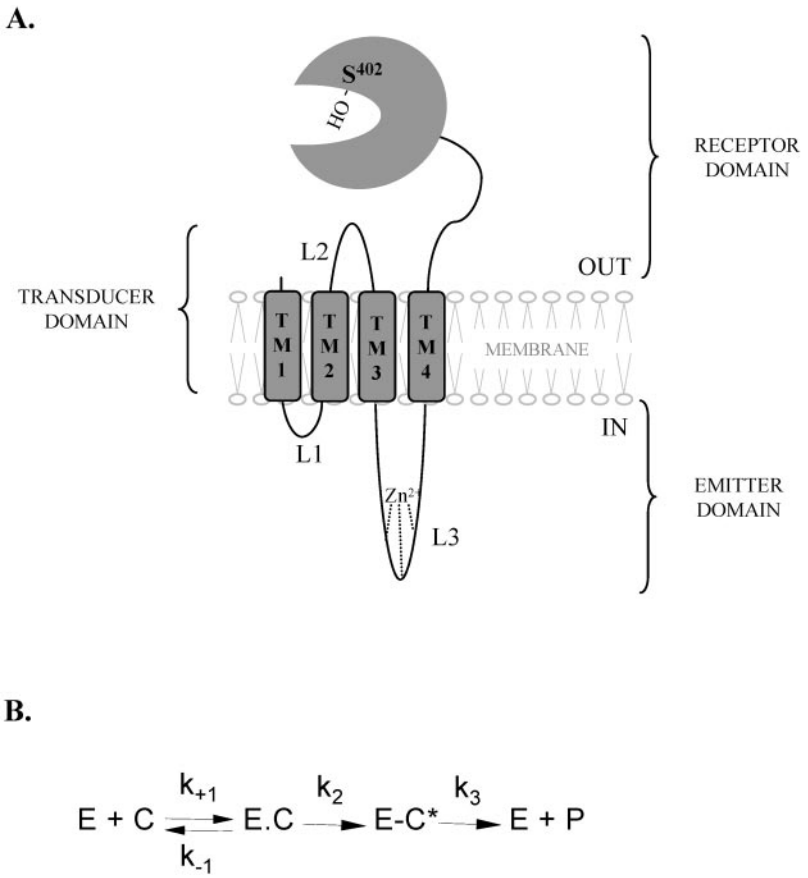

FIG. 1. *A*, membrane topology of the penicillin-sensory transducer, BlaR1. This receptor is a bipartite protein including an extracellular CTD and NTD. BlaR-CTD contains the three motifs of the penicilloyl serine transferase family ($S^{*402}TYK$, $Y^{476}GN$, $K^{539}TG$, where S^{402} is the active-site serine). BlaR1 is embedded in the plasma membrane via four transmembrane segments (TM1, TM2, TM3, and TM4). The extra- and intracellular loops connecting these segments are designated L1, L2, and L3. The cytoplasmic L3 loop contains a metalloprotease motif (zinc-binding site). *B*, interaction between an active-site serine penicillin-recognizing enzyme and a β-lactam antibiotic. *E* is the enzyme, *C* the β-lactam, *E.C* is the Henri-Michaelis complex, *E-C** is the acyl-enzyme, and *P* is the product of hydrolysis.

TM4). This topology defines three loops named L1, L2, and L3 connecting these hydrophobic segments. L1 and L3 are exposed in the cytoplasm, whereas L2 is outside the cell. The cytoplasmic L3 loop contains an HEXXH motif that is the signature of the thermolysin family of the Zinc metalloproteases (12, 17). This motif is directly involved in the cytoplasmic signal transmitted by BlaR1.

According to the proposed mechanism of signal transduction by BlaR1, acylation of the BlaR-CTD domain by β-lactam inducers generates a proteolytic activation of the intracellular metalloprotease. Two mechanisms for the inactivation of the BlaI repressor have been described. Zhang *et al.* (17) proposed a direct proteolysis of BlaI by the acylated BlaR1 receptor in *S. aureus*, whereas Filée *et al.* (7) concluded that the generation of a coactivator by the activated BlaR1 receptor in *B. licheniformis* combined with a cellular penicillin stress were necessary for BlaI inactivation. Binding of the antibiotics to the *S. aureus* BlaR-CTD generates a significant conformational change, and this process was proposed to play a role in the signal transduction process (16). Whatever the mechanism, BlaR-CTD is responsible for the sensing of the β-lactam antibiotic outside the cell and BlaR-NTD for the first signaling step in the cytoplasm. The transmission of the presence of the antibiotic detected by BlaR-CTD to BlaR-NTD requires a close interaction between these two domains. In BlaR-NTD, the 63-residue L2 extracellular loop connecting TM2 and TM3 is the best candidate to interact with BlaR-CTD (Fig. 1A). In this study, we investigated the interaction between L2 loop and BlaR-CTD by phage display. The conformational change of BlaR-CTD concomitant to its acylation by β-lactam antibiotics is probed by fluorescence spectroscopy, CD, and FTIR spectroscopy.

EXPERIMENTAL PROCEDURES

Bacterial Strains and Growth Conditions—E. coli DH5α and TG1 F′ strains (BD Biosciences Clontech) were used as hosts for cloning and phage amplification, respectively. Luria-Bertani broth and agar plates were used for growth of *E. coli* strains. When required, appropriate antibiotics were added to the media (100 μg/ml ampicillin or 7 μg/ml tetracycline).

Production of BlaR-CTD—BlaR-CTD was cloned, expressed, and purified as described previously (13).

Construction of the Phage fd-tet-DOG-L2—The DNA sequence encoding the L2 loop (Pro^{53} to Ser^{115} residues, *l2-loop*) of *B. licheniformis* BlaR1 was amplified by PCR using pRTW8 (14) as template and fd-tet-DOG1-L2up (5′-AGTGCACAGTGTGGTGGTCCTTTTATCCCCTTTCATTTTC-3′) and fd-tet-DOG1-L2rp (5′-TGCGGCCGCACACCCCCCTGAATCTATCATTTTGGAAGACG-3′) as amplimers. The oligonucleotides contained ApaLI or NotI site (underlined in the oligonucleotide sequences) to facilitate the cloning and introduced four and three additional codons, encoding Gln-Cys-Gly-Gly and Gly-Gly-Cys, at the 5′- and the 3′-ends of the *l2-loop*, respectively. The PCR fragment was ligated into the pCR 2.1 vector (Invitrogen), generating pCIP351. This plasmid was digested with ApaLI and NotI, and the fragment carrying *l2-loop* was cloned into the corresponding sites of the replicative form of the fd-tet-DOG1 phage (18, 19). In the resulting phage, fd-tet-DOG1-L2, the *l2-loop* was fused with the 5′ end of the fd-tet-DOG1 gene encoding the G3p protein to generate the *l2-loop-g3p* gene under the control of the P_{G3p} promoter. The fidelity of PCR and the final *l2-loop-g3p* fusion were confirmed by DNA sequencing.

Preparation of Phage Particles—E. coli TG1 F′ cells harboring fd-tet-DOG1 and fd-tet-DOG1-L2 were grown for 78 h at 23 °C on Luria-Bertani medium supplemented with 7 μg/ml tetracycline. Concentrated phage solutions were prepared by polyethylene glycol precipitations as previously reported by Legendre *et al.* (20). The number of phage particles per unit volume was determined from absorbance at 265 nm. One unit of absorbance corresponds to a solution of 7×10^{12} phage particles/ml.

SDS-PAGE and Western Blotting—Phage particles (10^{11} particles/20 μl) diluted in protein-denaturing buffer containing dithiothreitol as reductant (60 mM Tris-HCl, pH 6.8, 25% glycerol, 2% SDS, and 100 mM

dithiothreitol) were denatured by incubation at 100 °C for 15 min and submitted to SDS-PAGE. After electrophoresis, the proteins were transferred from the gel onto a nitrocellulose membrane (Millipore). Incubation of membrane with primary antibody (mouse monoclonal anti-G3p; Eurogentec) was followed by incubation with alkaline phosphatase-conjugated anti-mouse as secondary antibody (Bio-Rad). The primary and the secondary antibodies were diluted 400- and 3000-fold, respectively, in Tris-buffered saline containing 1% (w/v) bovine serum albumin and 0.5% (v/v) Tween 20. The immunocomplexes were detected by using nitro blue tetrazolium/5-bromo-4-chloro-3-indolyl phosphate chemistry (Roche Applied Science) as recommended by the manufacturer.

Phage ELISA—Microtiterplate wells (Kartell) were coated overnight at 4 °C with 5 μg of BlaR-CTD in 0.2 ml of PBS (50 mM phosphate buffer, pH 7.0, and 150 mM NaCl). After PBS washing (3 times with 300 μl), the wells were blocked with 300 μl of PBS buffer containing 2% (w/v) skim milk powder for 1 h at room temperature. 100 μl of the phage suspension (7×10^{11} phages/ml) were added and incubated for 1 h at room temperature. After incubation, the plates were washed (five times with 300 μl of PBS and 0.1% Tween 20 (PBST) and one time with 300 μl of PBS buffer containing 2% (w/v) skim milk powder) and incubated with anti-G8p major coat protein antibodies conjugated to horseradish peroxidase (Bio-Rad) at a 1:5000 dilution in PBS buffer containing 2% (w/v) skim milk powder. After extensive washing (five times with PBST and 1 time with PBS) bound phages were quantified using 2′2′-azinobis(3-ethylbenzthiazoline)sulfonic acid in the presence of H_2O_2 according to the manufacturer (Pharmacia). Absorbance readings were taken at 405 nm after 30 min. Some assays were also performed in the presence of β-lactam antibiotics. In this case, immediately after BlaR-CTD coating, plates were incubated with penicillin G (36 μg/ml final) or 6-APA (final concentration, 20 μg/ml) for 5 min at room temperature. Finally, some assays were performed in the absence of antibiotic as described above, except that the washing steps after the phage binding incubation were realized with PBS and Tween 20 containing 6-APA (20 μg/ml).

Fluorescence Experiments and Acrylamide Quenching Studies—Fluorescence measurements of free or acylated BlaR-CTD, were performed on an LS50 spectrofluorometer (PerkinElmer Life and Analytical Sciences), using a cell with a 1-cm light path. Fluorescence emission spectra in the 300–440 nm range were recorded using excitation wavelengths at 280 or 295 nm. The bandwidths for excitation and emission were 4 and 5 nm, respectively. At least 10 scans were averaged, and the appropriate blanks (buffer or buffer + antibiotic) were subtracted to obtain the corrected spectra.

Acrylamide quenching experiments were carried out at an excitation wavelength of 280 nm. Quenching measurements were made on five solutions of free or acylated BlaR-CTD containing increasing amounts of acrylamide (final concentration, 50–250 mM). Fluorescence intensities were measured at 340 nm after each addition of the quencher. The data were analyzed according to the modified Stern-Volmer equation: $F_O/F = (1 + K_{SV}[Q])e^{V[Q]}$, where K_{SV} is the Stern-Volmer constant for the dynamic quenching process, V is the static quenching constant, and $[Q]$ is the molar concentration of quencher. F_O and F represent the fluorescence intensities in the absence and the presence, respectively, of quencher. The values of K_{SV} and V were obtained by nonlinear regression using the Grafit software (Erithacus Software).

Before recording the spectra of the acylated protein, BlaR-CTD (1 μM) was incubated with penicillin G (10 μM) for 15 min at 37 °C. All measurements were carried out at 25 °C in 50 mM sodium phosphate buffer, pH 8.0.

CD Experiments—CD spectra were acquired with the help of a Jobin-Yvon CD6 spectropolarimeter using 0.2- and 1-cm path-length cells in the far (190–250 nm) and near (250–320 nm) UV, respectively. The CD spectra of free and acylated BlaR-CTD (4 or 80 μM in 50 mM sodium phosphate buffer, pH 8.0) were recorded at 25 °C and with a 2-nm bandwidth. The average from five scans was taken, and spectra were corrected for the blank by subtraction of the solvent spectrum obtained under identical conditions. Before recording the spectra of penicillin-acylated BlaR-CTD, the protein was incubated with penicillin G for 15 min at 37 °C and an antibiotic/protein molar ratio of 10.

Attenuated Total Reflection Fourier Transform IR Spectroscopy—Attenuated total reflection-FTIR spectroscopy spectra were recorded at room temperature on a Bruker IFS-55 IR spectrometer equipped with a liquid nitrogen-cooled mercury-cadmium-tellurium detector at a resolution of 4 cm^{-1}. The spectrophotometer was continuously purged with dry air. The internal reflection element (attenuated total reflection) was a germanium plate (50 × 20 × 2 mm; Harrick EJ2121) with an aperture angle of 45°, yielding 25 internal reflections (21).

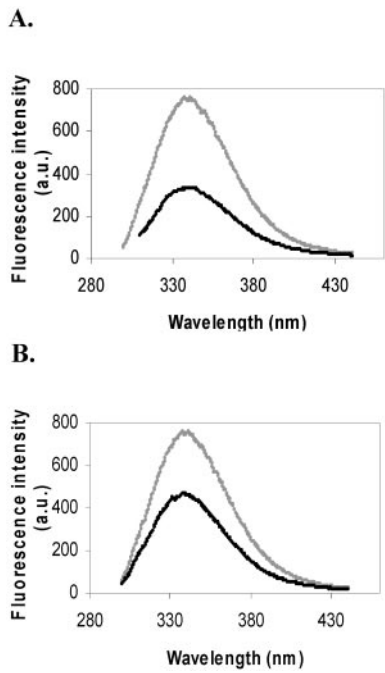

FIG. 2. **Fluorescence emission spectra of BlaR-CTD.** *A*, with excitation wavelength at 280 nm (*gray*) and 295 nm (*black*). *B*, free (*gray*) and penicilloylated BlaR-CTD (*black*) with excitation wavelength at 280 nm. All spectra were acquired in 50 mM sodium phosphate buffer, pH 8.0, at 25 °C. The BlaR-CTD and penicillin G concentrations were 1 and 10 μM, respectively.

Thin protein films were obtained by slowly evaporating a sample containing 70 μg of BlaR-CTD (in 100 μl of 50 mM sodium phosphate buffer, pH 8.0) on one side of the attenuated total reflection plate under a stream of nitrogen (22, 23). Before evaporating the acylated BlaR-CTD, the protein was incubated with a 10-fold molar excess of ampicillin for 15 min at 37 °C.

The determination of the secondary structure was based on the vibrational bands of the protein, particularly the amide I band (1600–1700 cm^{-1}), which is sensitive to the secondary structure. The analysis was performed on the amide I region of BlaR-CTD in the absence and presence of ampicillin. For each spectrum, 512 scans were averaged. Fourier self-deconvolution was applied to increase the resolution of the spectra in the amide I region. The self-deconvolution was carried out using a Lorentzian line shape for the deconvolution and a Gaussian line shape for the apodization. The area of the different components of amide I revealed by self-deconvolution was calculated as described by Goormaghtigh *et al.* (22).

Kinetics of Hydrogen-Deuterium Exchange—Films containing 70 μg of free or acylated BlaR-CTD were prepared on a germanium plate as described above. Samples were deuterated under a stream of D_2O-saturated nitrogen gas inside the sealed sample holder. The kinetics of hydrogen-deuterium exchange of amide protons was followed by monitoring the decreasing area of amide II and the increasing area of amide II′ as described by Goormaghtigh *et al.* (24). Twelve spectra were recorded and averaged for each kinetic time point. The areas of amide II and II′ bands were finally normalized between 0 and 100% for each time point.

RESULTS

BlaR-CTD Conformational Changes—The putative BlaR-CTD conformational changes after acylation by a β-lactam antibiotic were probed using a combination of spectroscopy techniques, including intrinsic fluorescence, fluorescence quenching by acrylamide, far-UV and near-UV CD, and FTIR spectroscopy.

Fluorescence Measurements—The BlaR-CTD polypeptide chain contains five tryptophan, 14 tyrosine, and 18 phenylalanine residues in its polypeptide chain. Excitation wavelengths of 280 and 295 nm yield different emission spectra (Fig. 2*A*), indicating that the tyrosine residues contribute significantly to the fluorescence spectra. Fig. 2*B* shows the intrinsic fluores-

cence emission spectra of free and acylated BlaR-CTD. In the presence of penicillin G, the fluorescence intensity decreases by about 37% without change in the position of the maximum emission wavelength at 340 nm. Similar results were obtained using ampicillin, another antibiotic inducer (data not shown). These results show that significant changes occur in the environment of least some of the aromatic residues upon β-lactam binding.

Quenching of Fluorescence by Acrylamide—Quenching of protein fluorescence by acrylamide offers a very useful method for monitoring protein conformation changes. The sensitivity of the quenching technique allows the detection of very subtle conformational rearrangements that accompany the binding of a ligand to a protein in terms of an increase or decrease in the exposure of tryptophan residues (25). This solvent accessibility is quantified by the Stern-Volmer plots presented in Fig. 3. The plots for free and acylated BlaR-CTD display upward curvatures, indicating significant contributions from both dynamic and static quenching. This is expressed by the modified Stern-Volmer equation (26): $F_O/F = (1 + K_{SV}[Q])e^{V[Q]}$, where K_{SV} is the Stern-Volmer constant for the dynamic quenching process and V is the static quenching constant. The values of K_{SV} and V are obtained by nonlinear regression of the data in Fig. 3. When penicillin G is added to BlaR-CTD, the K_{SV} drops from 4.4 ± 0.75 to 2.4 ± 0.23 M^{-1}. These values indicate that some tryptophan residues of BlaR-CTD are less exposed to acrylamide after antibiotic binding. The V values in the absence or presence of penicillin G are identical within experimental error (1.5 ± 0.39 and 1.6 ± 0.15 M^{-1}, respectively). Furthermore, the nonzero V values in all experimental conditions suggest that acrylamide binds near the aromatic residues and induces static quenching. To confirm that this fluorescence quenching is not caused by three-dimensional rearrangement, CD experiments in the far and near UV were performed.

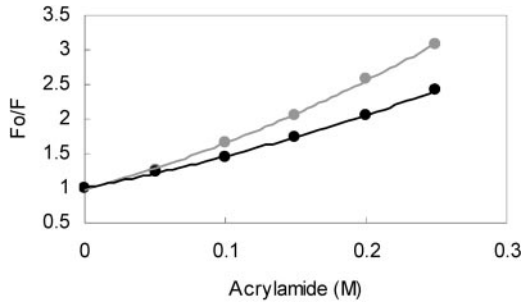

FIG. 3. **Stern-Volmer plots of F_O/F *versus* quencher concentration for free (*gray*) or acylated (*black*) BlaR-CTD.** F and F_O are the fluorescence intensities in the presence and absence of acrylamide, respectively. Experimental conditions were the same as for intrinsic fluorescence measurements. Spectra were recorded with excitation and emission wavelengths of 280 and 340 nm, respectively.

CD Studies—Far-UV spectra (190–250 nm) of free and acylated BlaR-CTD were recorded. After correction by substraction of the solvent spectra with or without penicillin G, both protein spectra are similar (Fig. 4*A*), indicating the absence of secondary structural change. The percentage of α-helix esti-

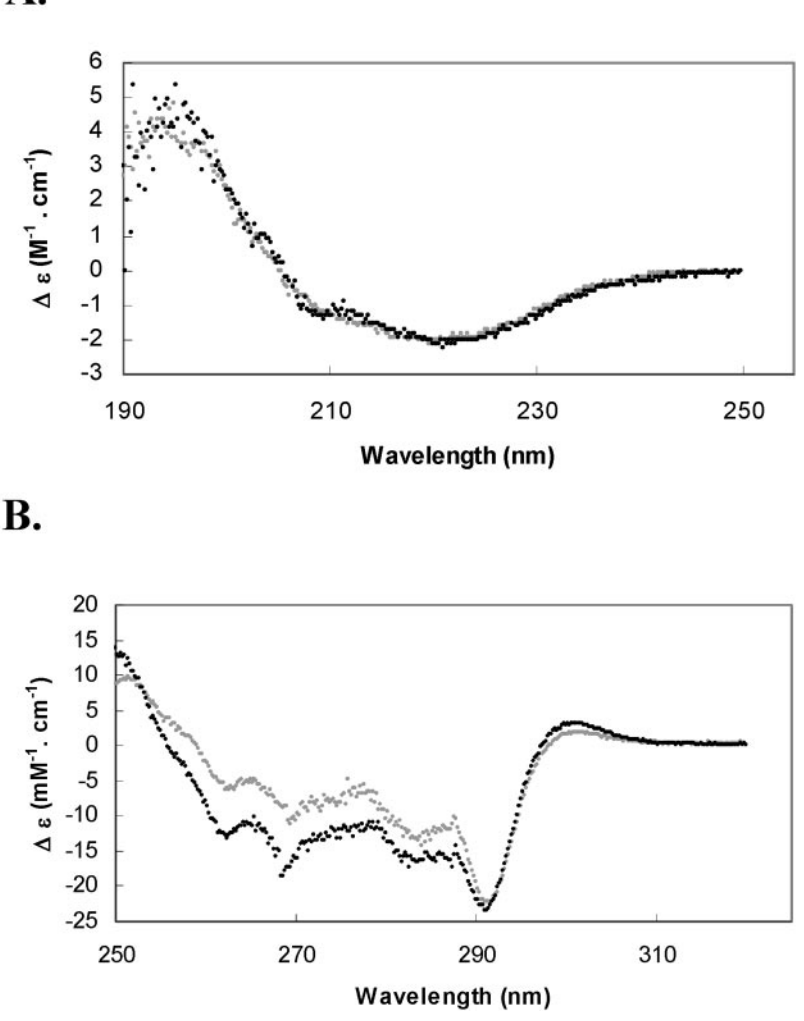

FIG. 4. **CD spectra of free (*gray*) or acylated (in *black*) BlaR-CTD.** *A*, in the far UV, BlaR-CTD and penicillin G concentrations were 4 and 40 μM, respectively. *B*, in the near UV, BlaR-CTD, and penicillin G concentrations were 8 and 80 μM, respectively. Spectra were recorded in 100 mM sodium phosphate buffer, pH 8.0, at 25 °C.

mated from far-UV CD is 60% (27). CD bands in the near-UV region (250–320 nm) originate from the aromatic amino acids. Therefore, the resultant near-UV CD spectrum is extremely sensitive to small changes in secondary and tertiary structures. The near-UV spectra of free and acylated BlaR-CTD are shown in Fig. 4B. In the absence of penicillin G, the spectrum shows a broad negative band with a minimum at 292 nm. Formation of the BlaR-CTD/penicillin G adduct results in a decrease in the ellipticity between 255 and 290 nm that is clearly apparent after subtraction of the contribution of the antibiotic. This indicates that the aromatic residues of the acylated BlaR-CTD are in a more asymmetric environment after antibiotic binding.

IR Spectroscopy: Secondary Structure Analysis—IR-attenuated total reflection spectra of free and acylated BlaR-CTD were recorded (data not shown). The amide I band, assigned to γ (C = O) of the peptide bond presents two absorption maxima around 1654 and 1632 cm^{-1}. The amide II band located around 1545 cm^{-1} is characteristic of the γ (N-H) of the peptide bond. The position of amide I at 1654 cm^{-1} indicates a relatively high amount of α-helix in the protein, and the low frequency shoulder near 1632 cm^{-1} indicates the presence of a significant proportion of β-sheet (22, 28). The shape of the amide I band for free and acylated BlaR-CTD is similar. The secondary structure of BlaR-CTD was analyzed from the shape of amide I after Fourier self-deconvolution and curve fitting as detailed in Goormaghtigh *et al.* (21) and consists of 58% α-helix, 29% β-sheet, and 13% turns. This α-helix value is in agreement with that obtained from CD measurements. Clearly, the secondary structure of BlaR-CTD does not change upon binding of antibiotic.

Deuterium/Hydrogen Exchange Kinetics—For a constant secondary structure and under identical experimental conditions, the rate of H/D exchange can be used as an indicator of tertiary structure changes. Kinetics of deuteration of free and acylated BlaR-CTD were monitored. The rate of amide H/D exchange is related to the solvent accessibility of the NH amide groups. Amide hydrogen exchange was followed by monitoring the amide II absorption peak as a function of the time of exposure to D_2O-saturated nitrogen. The percentage of exchange was computed between 0 and 100%. The decrease of the amide II region is proportional to the number of hydrogens that have been exchanged by deuterium and provides a probe of conformational changes. H/D exchange is shown in Fig. 5 as a function of deuteration time. The percentage of deuterium-hydrogen exchange is not significantly affected by antibiotic binding. H/D exchange is extremely rapid in the two tested situations; a large decrease of the amide II band intensity is observed during the first 3 min of exposure to D_2O, indicating a rapid replacement of a large number of amide hydrogens by deuterium. H/D exchange is much slower over the subsequent 60 min. Finally, more than 50% of the hydrogens do not exchange, according to the compact globular 3D structure of BlaR-CTD (29).

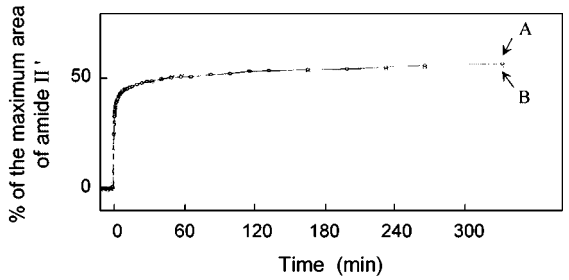

FIG. 5. **Percentage of exchanged amide hydrogens computed between 0 and 100% as a function of the deuteration time for the BlaR-CTD.** *A*, free BlaR-CTD; *B*, acylated BlaR-CTD. Spectra were recorded with a 70-μg film of BlaR-CTD and an ampicillin/BlaR-CTD molar ratio of 10.

Display of the L2 Loop—Phage display of the *B. licheniformis* BlaR1 receptor L2 loop was performed by fusion to the minor coat protein (G3p) to determine whether the L2 loop interacts with the BlaR-CTD. The L2 loop displayed at the N terminus of G3p and exhibiting two additional cysteines at its extremities can potentially form a disulfide loop (30, 31) (Fig. 6). The disulfide bond constrains the two extremities of the L2 loop in neighboring position as expected from the four-α-helix bundle model of BlaR-NTD (12).

The sequence encoding the L2 loop in fd-tet-DOG1-L2 phage were sequenced and shown to encode L2 loop fused in frame with G3p. The proteins of the coat of the phage fd-tet-DOG1 and fd-tet-DOG1-L2 were analyzed by Western blotting with antibodies against G3p (Fig. 7). A band of 70 kDa was seen for the fd-tet-DOG1 phage (an abnormal position was already observed by McCafferty *et al.* (32)) and a band at 77 kDa for the fd-tet-DOG1-L2. This showed that the L2 loop was fused to G3p on the phage coat and indicated that no significant proteolytic cleavage of the L2 loop occurred during the virus morphogenesis.

Expression of L2 loop on the phage surface results in a reduction in phage infectivity from 3.0 to 1.6%. This makes titration of infectious particles inappropriate for comparing the quantities of fd-tet-DOG1 and fd-tet-DOG1-L2 (33). For this reason, the amount of phage particles was expressed with respect to the total number of phage particles, rather than to the number of infectious phage and was determined by measuring absorbance at 265 nm.

Retention of the Phage—To analyze the interaction between

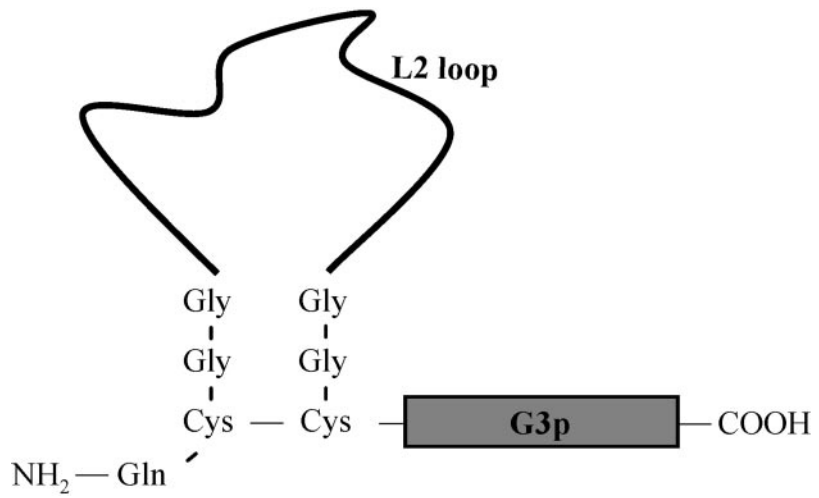

FIG. 6. **Schematic representation of the L2 loop-G3p fusion protein.** By choosing suitable PCR primers in the amplification of the *B. licheniformis* BlaR1 L2 loop coding sequence, L2 loop (Pro^{53} to Ser^{115}) was fused to the N terminus of the mature G3p coat protein of the phage fd-tet-DOG1. Three or four codons corresponding to Gln-Cys-Gly-Gly and Gly-Gly-Cys were added at the N- and C-terminal ends of L2 loop, respectively, connecting the L2 loop extremities by a disulfide bond.

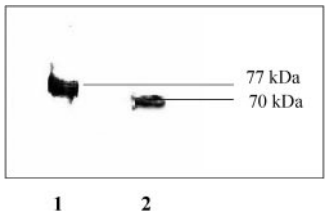

FIG. 7. **Western blot analysis of L2 loop-G3p fusion protein.** Denatured proteins from 10^{12} phages were loaded on a SDS-10% (w/v) polyacrylamide gel, separated by electrophoresis, and transferred onto a nitrocellulose membrane. The G3p and L2 loop-G3p proteins were revealed by a rabbit monoclonal anti-G3p antibody followed by an anti-rabbit antibody coupled to alkaline phosphatase. *Lane 1*, fd-tet-DOG1-L2; *lane 2*, fd-tet-DOG1.

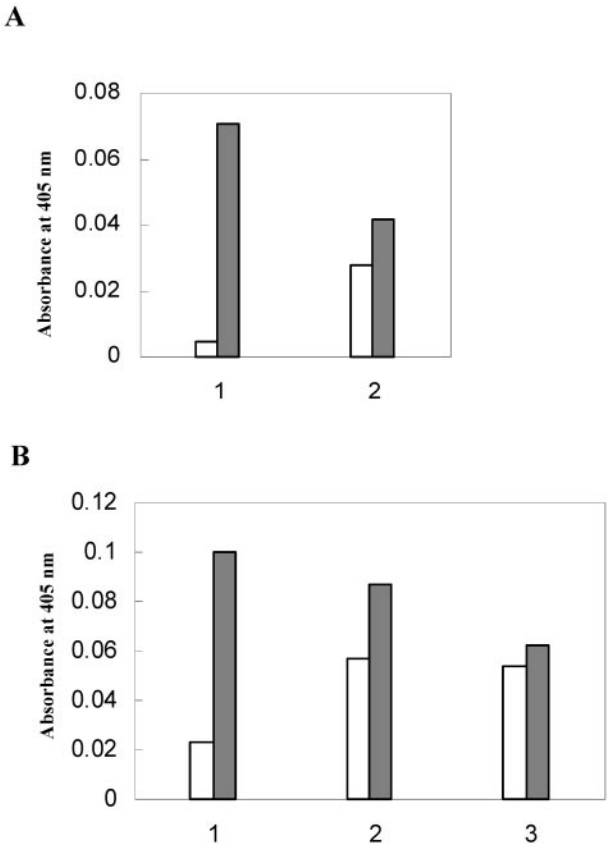

FIG. 8. **Interaction between the L2 loop and the BlaR-CTD as tested by ELISA.** BlaR-CTD coated onto an ELISA plate can be expected to interact with the L2 loop present on the phage surface. Fd-tet-DOG1-L2 phage (*gray bars*) was compared with fd-tet-DOG1 phage used as a control (*white bars*). *A*, ELISA in presence of penicillin G (35 μM). *Lane 1*, free BlaR-CTD. *Lane 2*, acylated BlaR-CTD. *B*, ELISA in presence of 6-APA (20 μM). *Lane 1*, free BlaR-CTD. *Lane 2*, acylated BlaR-CTD. *Lane 3*, as *lane 1* except that washing steps after phage binding incubation were realized in presence of 6-APA (20 μM). The values are the means of triplicate experiments and experimental errors are below 10%.

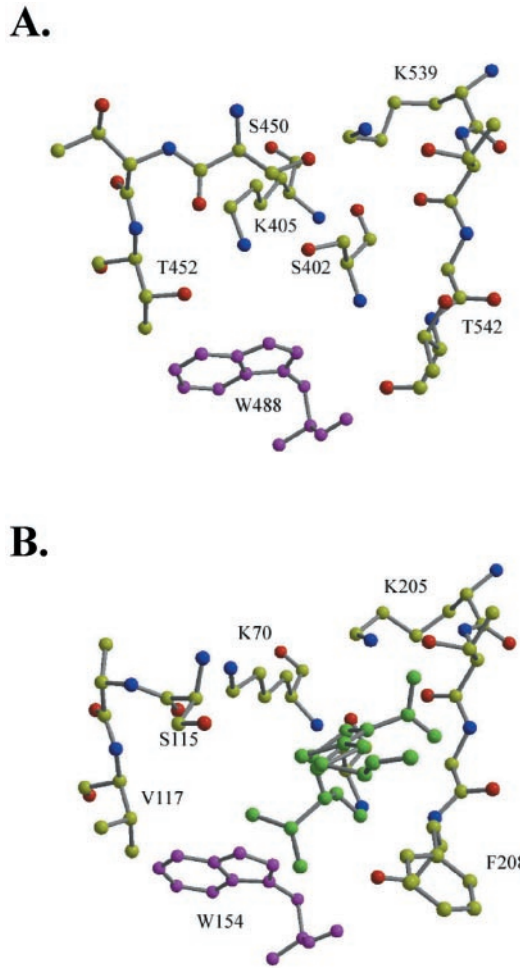

FIG. 9. **Comparison of the active sites of BlaR-CTD (*A*) and of the class D β-lactamase OXA-13 in the presence of imipenem (*B*).** Trp^{488} of BlaR-CTD and the equivalent Trp^{154} of OXA-13 (in *magenta*) point into the active site. Trp^{154} of OXA-13 does not directly interact with imipenem (in *green*) but its environment is modified by the presence of the antibiotic.

L2 loop and BlaR-CTD, a phage ELISA was designed. This ELISA yields an absorbance value proportional to the amount of bound phages. Phages displaying the L2 loop were significantly retained on the ELISA plates coated with BlaR-CTD (Fig. 8*A*). Indeed fd-tet-DOG1-L2 phages are 15-fold more adsorbed than fd-tet-DOG1 control phages. When BlaR-CTD is acylated by penicillin G, the retention of fd-tet-DOG1-L2 phages becomes similar to that observed with the control phages, but adsorption of the control phages is increased. The experiment was repeated using 6-APA as an acylation agent (Fig. 8*B*) with similar results. Adsorption of the fd-tet-DOG1-L2 phages was significantly higher than that of the control phages (Fig. 8*B1*) and after acylation of BlaR-CTD, the difference became not significant but the background level was increased (Fig. 8*B2*). With the free BlaR-CTD, addition of 6-APA in the washing buffer resulted in a complete disappearance of the difference between phages displaying L2 loop and control phages (Fig. 8*B3*). These results demonstrate an interaction between the L2 loop and the BlaR-CTD soluble domain. If BlaR-CTD is penicilloylated this interaction does not occur.

DISCUSSION

Transmembrane receptors are proteins through which cells commonly receive information from the outside and transmit it for processing into the cytoplasm. Typical receptor contains an extracellular ligand binding domain, a cytoplasmic signaling domain, and transmembrane hydrophobic sequences. The mechanism by which external ligand binding generates an intracellular signal is poorly understood. For the aspartate receptor of chemotaxis, it was suggested that conformational changes caused by the ligand binding at the dimer interface induce a relative realignment of the helices at the interface, thus transmitting conformational information from the periplasm to the cytoplasm (34). In a first approach, we have explored a putative conformational change in the penicillin-

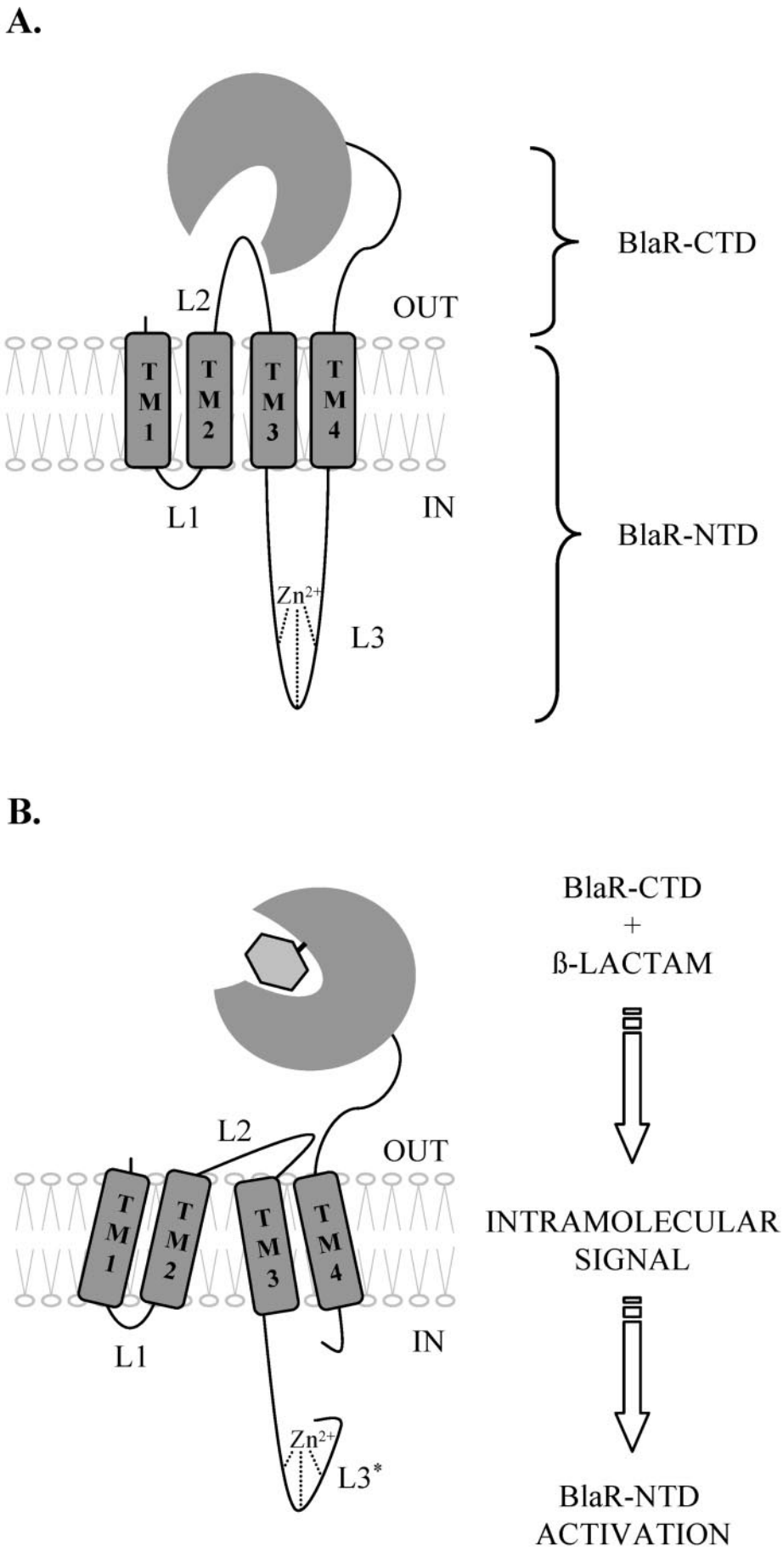

FIG. 10. **Tentative model explaining signal transduction by the *B. licheniformis* BlaR1.** *A*, in the absence of β-lactam antibiotic, BlaR-CTD interacts with the extracytoplasmic L2 loop. This interaction constrains the four transmembrane segments (TM1–TM4) to adopt relative positions such that the intracellular L3 loop remains inactive. *B*, BlaR-CTD acylation entails a release of the BlaR-CTD/L2 loop interaction, resulting in motion of the transmembrane segments and activation of L3 loop metalloprotease.

binding domain of the *B. licheniformis* BlaR1 receptor after binding of a β-lactam antibiotic.

Far-UV CD and IR spectra are extremely sensitive to small changes in secondary structures. They were used as probes for small conformational changes in the BlaR-CTD structure after binding β-lactam antibiotics. Clearly, antibiotic binding does not significantly modify the secondary structure of BlaR-CTD. In *S. aureus*, by contrast, a significant conformational change of BlaR-CTD upon acylation by β-lactam antibiotics was reported in terms of enhancement of secondary structure (α-helicity and β-sheets) (16).

Near-UV CD, fluorescence, and, for a constant secondary structure, FTIR spectroscopies can be used as indicators of tertiary structure changes. Near-UV CD spectra of free and acylated BlaR-CTD show a significant difference in the environment of the aromatic residues. BlaR-CTD contains many aromatic residues, and they all contribute to the spectrum to various extents. It is thus difficult to interpret a small change in the spectrum in structural terms, because any of many chromophores might be responsible for the spectral modifications. Similar conclusions are deduced from fluorescence emission spectra of free and acylated BlaR-CTD. When BlaR-CTD is acylated, fluorescence intensity decreases by 37% without change in the position of the maximum. Studies of fluorescence quenching demonstrate that some tryptophan residues of BlaR-CTD are becoming less exposed to acrylamide upon antibiotic binding. There are two possible explanations for this decrease in tryptophan indole exposure upon antibiotic binding. First, the antibiotic itself might act sterically to shield Trp^{488} residue from collision with acrylamide. Indeed, the crystal structure of BlaR-CTD shows that the Trp^{488} residue points into the active site of BlaR-CTD (Fig. 9*A*; Protein Data Bank code 1NRF) (29). In the class D β-lactamase OXA-13, the equivalent Trp^{154} also points into the active site and, clearly, its environment is modified by imipenem binding (Fig. 9*B*; Protein Data Bank code 1H5X). The other explanation is that antibiotic binding induces a widespread conformation change in BlaR-CTD, resulting in a slight decrease in the exposure of several fluorescent residues.

Amide H/D exchange, followed during the time of exposure of the sample to D_2O-saturated nitrogen, allows us to determine the accessibility of the amide hydrogens to the solvent and provides a measure of tertiary conformational change. The kinetics of deuteration of free and acylated BlaR-CTD were similar. These data indicate that free and acylated BlaR-CTD have the same general conformation. In addition, the structures of the other PBPs (*Streptococcus pneumoniae* PBP2a (35); *S. aureus* PBP2a (36)) did not reveal important conformation changes after antibiotic binding. According to these observations, then, it is reasonable to conclude that the β-lactam antibiotic does not induce a drastic conformation change in *B. licheniformis* BlaR-CTD.

Consequently, signal transduction by BlaR1 from the outer side of the membrane to the cytoplasmic compartment should require interactions between the penicillin-binding CTD and NTD. To analyze the interaction between the two domains of the *B. licheniformis* penicillin receptor BlaR1, a phage ELISA was designed. We have shown that phages displaying L2 loop can significantly interact with BlaR-CTD. The low signal suggests a weak interaction between the two domains of BlaR1. Phage ELISAs allow us to investigate both strong and weak interactions. It was reported that a K_d value as low as 0.1 mM can be detectable (37). When BlaR-CTD is acylated by either penicillin G or 6-APA, phages expressing the L2 loop did not appear to bind to BlaR-CTD because there was no increase in signal intensity compared with control phage. The binding of the phages in the presence of penicillin G seems to lead to some nonspecific binding of the phages to the wells, as suggested by the increased background level. We attempted to minimize this nonspecific interaction by using 6-APA that has no hydrophobic lateral chain in contrast penicillin G. In this case, we also observed nonspecific binding of the control phage. Nonetheless, BlaR-CTD acylated by 6-APA has lost its capacity to interact with the L2 loop because there is no significant retention of phages displaying L2 loop. Moreover, addition of 6-APA in the washing solution leads to displacement of the bound phages by loss of the L2 loop/BlaR-CTD interaction. According to these results, we propose the following hypothesis. In the absence of β-lactam antibiotic (inducer), the BlaR-CTD domain interacts with the L2 loop. This interaction constrains the four transmembrane segment TM1–TM4 to adopt relative positions so that the intracellular L3 loop remains inactive. When a β-lactam antibiotic is present in the outer medium, BlaR-CTD is acylated. This triggers a release of the L2 loop/BlaR-CTD interaction, causing a motion of the transmembrane helices and transduction of the information into the cytoplasm, involving activation of L3 loop metallopeptidase (Fig. 10). In *S. aureus*, deletion of the BlaR-CTD 35 C-terminal amino acids results on constitutive β-lactamase synthesis (38). In this truncated BlaR-CTD, the L2 loop/BlaR-CTD interaction is lost as in the native BlaR-CTD after acylation by a β-lactam antibiotic. Meanwhile, when only BlaR-NTD domain is present, there is no β-lactamase induction (29). Thus, BlaR-CTD naturally imposes constraints onto the transmembrane regions outside the L2 loop/BlaR-CTD interaction that permits the correct folding of the intracellular L3 loop.

Acknowledgment—We thank Dr. E. Sauvage for Fig. 9.

REFERENCES

1. Joris, B., Hardt, K., and Ghuysen, J. M. (1994) in *Bacterial Cell Wall* (Ghuysen, J. M., and Hakenbeck, R., eds) Vol. 27, pp. 505–515, Elsevier Science publishers B. V., Amsterdam
2. Philippon, A., Dusart, J., Joris, B., and Frère, J. M. (1998) *Cell. Mol. Life Sci.* **54,** 341–346
3. Salerno, A. J., and Lampen, J. O. (1988) *FEBS Lett.* **227,** 61–65
4. Clarke, S. R., and Dyke, K. G. (2001) *Microbiology* **147,** 803–810
5. Kobayashi, T., Zhu, Y. F., Nicholls, N. J., and Lampen, J. O. (1987) *J. Bacteriol.* **169,** 3873–3878
6. Hackbarth, C. J., and Chambers, H. F. (1993) *Antimicrob. Agents Chemother.* **37,** 1144–1149
7. Filée, P., Benlafya, K., Delmarcelle, M., Moutzourelis, G., Frère, J. M., Brans, A., and Joris, B. (2002) *Mol. Microbiol.* **44,** 685–694
8. Sherratt, D. J., and Collins, J. F. (1973) *J. Gen. Microbiol.* **76,** 217–230
9. VanMelckebeke, H., Vreuls, C., Gans, P., Filée, P., Llabres, G., Joris, B., and Simorre, J. P. (2003) *J. Mol. Biol.* **333,** 711–720
10. Garcia-Castellanos, R., Marrero, A., Mallorqui-Fernandez, G., Potempa, J., Coll, M., and Gomis-Ruth, F. X. (2003) *J. Biol. Chem.* **278,** 39897–39905
11. McKinney, T. K., Sharma, V. K., Craig, W. A., and Archer, G. L. (2001) *J. Bacteriol.* **183,** 6862–6868
12. Hardt, K., Joris, B., Lepage, S., Brasseur, R., Lampen, J. O., Frère, J. M., Fink, A. L., and Ghuysen, J. M. (1997) *Mol. Microbiol.* **23,** 935–944
13. Duval, V., Swinnen, M., Lepage, S., Brans, A., Granier, B., Franssen, C., Frère, J. M., and Joris, B. (2003) *Mol. Microbiol.* **48,** 1553–1564
14. Joris, B., Ledent, P., Kobayashi, T., Lampen, J. O., and Ghuysen, J. M. (1990) *FEMS Microbiol. Lett.* **58,** 107–113
15. Gregory, P. D., Lewis, R. A., Curnock, S. P., and Dyke, K. G. (1997) *Mol. Microbiol.* **24,** 1025–1037
16. Golemi-Kotra, D., Cha, J. Y., Meroueh, S. O., Vakulenko, S. B., and Mobashery, S. (2003) *J. Biol. Chem.* **278,** 18419–18425
17. Zhang, H. Z., Hackbarth, C. J., Chansky, K. M., and Chambers, H. F. (2001) *Science* **291,** 1962–1965
18. Clackson, T., Hoogenboom, H. R., Griffiths, A. D., and Winter, G. (1991) *Nature* **352,** 624–628
19. Soumillion, P., Jespers, L., Bouchet, M., Marchand-Brynaert, J., Winter, G., and Fastrez, J. (1994) *J. Mol. Biol.* **237,** 415–422
20. Legendre, D., Laraki, N., Graslund, T., Bjornvad, M. E., Bouchet, M., Nygren, P. A., Borchert, T. V., and Fastrez, J. (2000) *J. Mol. Biol.* **296,** 87–102
21. Goormaghtigh, E., Cabiaux, V., and Ruysschaert, J. M. (1990) *Eur. J. Biochem.* **193,** 409–420
22. Goormaghtigh, E., Cabiaux, V., and Ruysschaert, J. M. (1994) *Subcell. Biochem.* **23,** 405–450
23. Fringeli, U. P., and Gunthard, H. H. (1981) *Mol. Biol. Biochem. Biophys.* **31,** 270–332
24. Goormaghtigh, E., Vigneron, L., Scarborough, G. A., and Ruysschaert, J. M. (1994) *J. Biol. Chem.* **269,** 27409–27413

25. Eftink, M. R., and Ghiron, C. A. (1976) *Biochemistry* **15,** 672–680
26. Eftink, M. R., and Ghiron, C. A. (1981) *Anal. Biochem.* **114,** 199–227
27. Greenfield, N., and Fasman, G. (1969) *Biochemistry* **8,** 4108–4116
28. Byler, D. M., and Susi, H. (1986) *Biopolymers* **25,** 469–487
29. Kerff, F., Charlier, P., Colombo, M. L., Sauvage, E., Brans, A., Frère, J. M., Joris, B., and Fonze, E. (2003) *Biochemistry* **42,** 12835–12843
30. McLafferty, M. A., Kent, R. B., Ladner, R. C., and Markland, W. (1993) *Gene* **128,** 29–36
31. Hoess, R. H. (1993) *Curr. Opin. Struct. Biol.* **3,** 572–579
32. McCafferty, J., Griffiths, A. D., Winter, G., and Chiswell, D. J. (1990) *Nature* **348,** 552–554
33. McCafferty, J., Jackson, R. H., and Chiswell, D. J. (1991) *Protein Eng.* **4,** 955–961
34. Milburn, M. V., Prive, G. G., Milligan, D. L., Scott, W. G., Yeh, J., Jancarik, J., Koshland, D. E., Jr., and Kim, S. H. (1991) *Science* **254,** 1342–1347
35. Gordon, E., Mouz, N., Duée, E., and Dideberg, O. (2000) *J. Mol. Biol.* **299,** 477–485
36. Lim, D., and Strynadka, N. C. (2002) *Nat. Struct. Biol.* **9,** 870–876
37. Rossenu, S., Dewitte, D., Vandekerckhove, J., and Ampe, C. (1997) *J. Prot. Chem.* **16,** 499–503
38. Lewis, R. A., Curnock, S. P., and Dyke, K. G. (1999) *FEMS Microbiol. Lett.* **178,** 271–275